sustainability

MDPI

Article

# How to Maintain a Sustainable Environment? A Spatial Evolution of Urban Atmospheric Pollution and Impact Factors in China

Mingze Li [1], Yuan Huang [1] and Mingdan Han [2,*]

[1] School of Management, Wuhan University of Technology, Wuhan 430070, China
[2] School of Entrepreneurship, Wuhan University of Technology, Wuhan 430070, China
* Correspondence: cyxy@whut.edu.cn

Received: 3 July 2019; Accepted: 8 August 2019; Published: 13 August 2019

**Abstract:** Urban pollution has significantly contributed to the spread of diseases and global warming. The analysis of spatial distribution characteristics of atmospheric pollutants is crucial for making sustainable industrial policy, and environmentally friendly urban planning. In this paper, GeoDa software is used to analyze how sulfur dioxide ($SO_2$), nitrogen oxides ($NO_x$), and smoke dust (DUS) are spatially distributed in various provinces of China. Then, global spatial correlation test and cluster analysis are carried out to obtain the spatial evolution characteristics of three pollutants. Afterward, the spatial panel data model is applied to explore the factors that affect the spatial evolution of $SO_2$, $NO_x$ and smoke dust (DUS) nationwide. MATLAB is used to estimate the Spatial Lag Model (SLM) and the Spatial Error Model (SEM) of the three pollutants, respectively. According to our analysis, SEM is more applicable for $SO_2$ and $NO_x$, whereas SLM is optimal for smoke dust (DUS). The results show that foreign direct investment (FDI), industrial structure, and urbanization aggravate environmental pollution, while per capita gross domestic products (per capita GDP) has a negative relationship with the cluster of pollutants. The study concludes by informing public policy makers on environment friendly policies for a more sustainable development.

**Keywords:** urban pollution; spatial evolution; spatial panel data model; sustainable development

## 1. Introduction

Environmental issues are a significant concern all over the world, especially in China. With the rapid development of China's current economy and its urbanization and industrialization, air pollution has become an increasingly severe problem, threatening human health and the sustainable development of countries [1,2]. This has drawn widespread concern about the spatial and temporal changes in air pollution [3]. Atmospheric pollutants can be divided into gaseous pollutants, which mainly include sulfur dioxide ($SO_2$) and nitrogen oxides ($NO_x$), and aerosol pollutants, commonly existed in the form of smoke dust (DUS). $SO_2$ can form particulate matter and acid rain, which leads to acidification of the soil, pollution of rivers, and corrosion of metals and buildings [4]. $NO_x$ is one of the main substances causing atmospheric acidification and the major source of ozone in the troposphere [5,6]. DUS can cause serious health issues and a reduction in urban atmospheric visibility [7,8]. Although the environmental quality has improved in recent years, due to the uneven economic development in different regions, different environmental problems have tangled up, which has seriously affected the healthy and sustainable development of China's economy. Therefore, an investigation into the spatial evolution of urban pollution in China and the factors influencing it is of great importance and significance.

Anthropogenic sources of air pollution include combustion products from energy production, motorized transportation, and household heating of wood, coal or oil, waste incineration, industrial emissions, and emissions from agricultural areas [9]. Scholars have studied the relationship between economic growth and pollution extensively. In the early 1970s, Georgescu believed that economic development would be at the expense of the environment [10], and economic growth would be subject to environmental constraints. Goeller and Weinberg and Dasgupta et al. disagreed and held the opinion that economic growth can be achieved without damaging the environment and technological advances will also help improve the environment [11,12]. After studying the relationship between environmental quality and per capita income, Grossman et al., pointed out that at low income levels, pollution increases with per capita gross domestic products (per capita GDP), and yet at high income levels, it declines with per capita GDP growth [13]. This inverted U-shaped relationship between environment quality and per capita income is called the Environmental Kuznets Curve [14]. The Environmental Kuznets Curve Theory (EKC) believes that in the early stage of economic development, pollutants are on the rise, but when the economy develops to a certain stage, the environment quality will be improved, hence presenting the inverted U-shaped process. Based on this, scholars have conducted extensive research. Ma et al. and Hao et al. supported the EKC hypothesis and analyzed the spatial spillover effects of economic activities on particulate matter smaller than 2.5 micrometers (PM2.5), and believed that there is an inverted U-shaped EKC in economic development in China [15,16], which, according to them, is an important factor affecting air pollution. Some scholars have studied the air pollution in different regions such as the Yangtze River Delta in China and the San Francisco Golden Valley in California from the aspects of urban form [17], land use [18], urbanization [19], and population density [20]; Han L et al. concluded that there is a significant positive correlation between urban population and secondary industry as well as air pollutant concentrations [21]. Yuan X et al. argued that economic development has a certain degree of impact on energy consumption and air environment, but it is not necessarily a negative impact [22]. In addition, previous research has focused on air pollution or human health impacts [23,24]. Most of the above literature neglect to investigate the dynamic evolution process of spatial distribution of atmospheric pollution. Moreover, most of the literature on factors influencing atmospheric pollution fails to compare the spatial distribution patterns of different pollutants, resulting in the difficulty in finding out the concrete impact factors of different pollutants. At present, air pollution continues to be a serious issue and governments are committed to reduce it by taking a series of measures. In this context, it is necessary to consider the distribution characteristics of various pollutants in a holistic manner to formulate a more reasonable policy on air pollution reduction.

Based on the above trends in literature, this paper uses GeoDa software to explore the spatial distribution characteristics of $SO_2$, $NO_x$, and DUS emissions in various provinces in China, and obtains the spatial evolution of these three pollutants from 2011 to 2017, which fills gaps in existing literature by emphasizing that the spatial distribution of air pollution is a dynamic process. At the same time, it compares and analyzes the three pollutants, and explores their distribution characteristics as a whole. We analyzed the relevant data obtained from provinces in China, and explored important factors influencing the spatial evolution of urban pollution by establishing a spatial weighted matrix and applying the spatial panel data model. Our study shows that the Spatial Error (SEM) model is more suitable for $SO_2$ and $NO_x$, whereas the Spatial Lag Model (SLM) model can achieve optimal results for DUS. This paper covers a wider range of regions and adds comparative analysis of the distribution characteristics of pollutants, which enriches existing literature in this field.

## 2. Method

### 2.1. Index Selection and Data Source

Using provincial administrative regions in China as spatial units, this paper intends to study the spatial patterns and evolution of three typical air pollutants, i.e., sulfur dioxide, nitrogen oxides, and smoke dust. Then, based on comparative analysis of the spatial patterns and evolution features of the three pollutants, we aimed to identify the key factors contributing to the emissions of each pollutant.

There are 34 provincial-level administrative regions in China. As spatial measurement analysis requires certain spatial connection among the spatial units and there are difficulties in obtaining data from Special Administrative Regions (i.e., Hong Kong, Macao, Taiwan), we cannot but excluded Hong Kong, Macao, Taiwan, and Hainan in the study. Therefore, we carried out our study by using the remaining 30 provincial regions as spatial units.

Data of the pollutants in this study are all obtained from China Statistical Yearbook, which is an annual statistical publication complied by the National Bureau of Statistics of China aimed at comprehensively reflecting the economic and social development of China. The latest issue of the yearbook is the 2018, which recorded the statistics of 2017. Meanwhile, some pollutant indicators are missing in the yearbooks before 2011. Because of these reasons, we selected $SO_2$, $NO_x$, and DUS data from 2011 to 2017 as our analysis samples.

In the selection of influencing factors found in existing literature, we have selected five types of influencing factors: industry location quotient (IND), proportion of urban population (URB), per capita (GDP), foreign direct investment (FDI), and population density (DEN) to investigate how they affect the emissions of different pollutants. Data on influencing factors are obtained from the Wind database. Among them, IND is the ratio of industrial outputs of each provincial region to that of the nationwide, reflecting industrial concentration and dispersion. Prior studies show that urban pollution is closely related to industrial structure [25,26]. Elhorst and Paul also indicate that industrial structure is the dominant factor affecting environmental patterns in China [27]. URB refers to the proportion of non-agricultural population in each provincial region. The level of urbanization also has a certain impact on climate pollutions [28]. Moreover, according to the Environmental Kuznets Curve Theory, per capita income is related to environment quality, so this paper selects the per capita GDP of each provincial region to indicate the economic growth. The "Pollution Haven Hypothesis" [29] states that countries with strict environmental standards seek to taking advantage of factories or industries in developing countries with lax environmental regulations, thereby transferring pollution to these countries and making them "pollution safe havens" for the developed countries [30,31]. Thus, this paper uses the amount of FDI in each provincial region to indicate the transfer of foreign industries. As population density might also affect air pollution [32–34]; we intend to examine its impact on pollution.

In all, we choose industry location quotient (IND), proportion of urban population (URB), per capita (GDP), foreign direct investment (FDI), and population density (DEN), and the emissions of sulfur dioxide ($SO_2$), nitrogen oxides ($NO_x$), and smoke dust (DUS) in 30 provincial regions in China from 2011 to 2017 as analysis samples, and the total data is 1680.

### 2.2. Method Selection

The empirical analysis is divided into two parts. The first part analyzes the spatial evolution characteristics of $SO_2$, $NO_x$, and DUS, produces quartile statistics, and then performs Moran's I and local Moran's I tests. The second part uses spatial panel data model to explore the connection between each influencing factor and the emission of the three pollutants, and then applies the maximum likelihood method to estimate the parameters and select the appropriate model [35].

#### 2.2.1. Analysis of Spatial Evolution Characteristics

The spatial evolution characteristics of the three pollutants: First, we used GeoDa software to plot the quartile statistics of $SO_2$, $NO_{x,}$ and DUS emissions, which can visualize the spatial characteristics of the three pollutants. The Moran's I test is performed to measure the global spatial correlation of the three pollutants. Moran's I is the correlation coefficient of the overall data, reflecting the spatial clusters and dispersion of the activities of the whole region. The scatter plots are applied to visualize the spatial characteristics of each provincial region. The formula of Moran's I is shown as follows:

$$\text{Moran's I} = \frac{\sum_{i=1}^{n}\sum_{j=1}^{m} W_{ij}\left(Y_i - \overline{Y}\right)\left(Y_j - \overline{Y}\right)}{S^2 \sum_{i=1}^{n}\sum_{j=1}^{n} W_{ij}} \quad (1)$$

In the formula, $S^2 = \frac{1}{n}\sum_{i=1}^{n}\left(Y_i - \overline{Y}\right)$; $S^2 = \frac{1}{n}\sum_{i=1}^{n}\left(Y_i - \overline{Y}\right)$. $Y_i$ is the observation value of the $i$-th geographic unit; $n$ is the total number of geographic units; $W_{ij}$ is a standard contiguity matrix. Moran's I ranges from −1 to 1. If the value is positive, it indicates a positive spatial correlation of the observed geographic units; if it is negative, there is a negative spatial correlation of the observed geographic units.

Next, the Local Indicators of Spatial Association (LISA) cluster analysis is performed to visualize the results of the local Moran's I. LISA are used to evaluate whether there are variables in local areas. The LISA of each geographic observation unit represents the spatial cluster of a given geographic observation unit with other similar units at a certain significance level. The sum of the LISA of all geographic observation units is related to Moran's I. Local Moran's I is expressed in the formula below:

$$\text{Moran's I}_i = Z_i \sum_{j=1}^{n} W_{ij} Z_j \quad (2)$$

In the formula, $W_{ij}$ is a spatial weight matrix. Moran's $\text{I}_i$ can be used to show that the observation value deviation $Z_i$ of the $i$-th geographic observation unit is multiplied by the weighted average value of the observation value deviation $Z_j$ of its neighboring unit j. If $Z_j > 0$, there are similar spatial clusters in the geographic observation units; otherwise the clusters are not similar [36].

### 2.2.2. Analysis of Spatial Panel Modeling

The second part explores the relationship between influencing factors and air pollution emissions by establishing spatial panel models, using MATLAB software and the maximum likelihood (ML) to estimate the parameters of the models. At the same time, log-likelihood (LogL), LM test and Robust LM test are conducted to select the optimal analysis model [37].

There are two commonly used spatial panel models, the Spatial Lag Model (SLM) and the Spatial Error Model (SEM). SLM is mainly used to study the effects of individuals in specific regions on the economic activities of geographically adjacent areas. SLM highlights the existence of spatial dependence in variables and it has a critical influence on the model and its spatial correlation. In SLM, the spatial correlation of explanatory variables is represented by spatially lagged explanatory variables, and the established model is as follows:

$$\text{LnV} = \beta_1\text{LnIND} + \beta_2\text{LnURB} + \beta_3\text{LnDEN} + \beta_4\text{LnFDI} + \beta_5\text{LnAGDP} + \rho\text{WLnV} + \varepsilon \quad (3)$$

In the model, WLnV is the spatially lagged explanatory variable, and $\rho$ is the spatial autoregressive coefficient. The estimated value and positive or negative of $\rho$ shows the geospatial correlations and directions (positive or negative). w is the spatial weight matrix for dimension, which is generated by using proximity relationship.

SEM is mainly used to capture the spatial interactions across different units, i.e., the errors of the established model are spatially correlated. When the spatial correlation is transmitted by other variables that are not estimated by the explanatory variables of the model, it can be determined that the spatial error is the cause for the spatial correlation, which is measured by SEM. The model is shown as follows:

$$\text{LnV} = \beta_1\text{LnIND} + \beta_2\text{LnURB} + \beta_3\text{LnDEN} + \beta_4\text{LnFDI} + \beta_5\text{LnAGDP} + \lambda\text{LnW}\mu + \varepsilon \quad (4)$$

In the model, LnIND, LnURB, LnDEN, LnFDI, LnAGDP represents the logarithmic of industry location quotient, proportion of urban population, and population density, foreign direct investment and per capita GDP respectively, $\lambda$ is the spatial error autocorrelation coefficient, and represents the spatial correlation between the regression residuals, $LnW\mu$ is the spatially lagged error term.

Due to the differences in the characteristics of pollutants, we cannot directly judge which spatial model is better. The following criteria can be used to select the appropriate model for analysis. The appropriate model can be determined by comparing the significance of the Lagrange Multiplier (LM) test first in the spatial correlation analysis. LM, proposed by Engle, is a statistical method used to test sequential correlation [38]. When the LM test values of SLM and SEM are significant further steps can be taken to compare the Robust LM-test value to determine the optimal model. LogL is the log likelihood value of the model. The larger the log likelihood value, the better the model fits.

### *2.3. Data Preprocessing*

This paper uses annual data from each provincial administrative region across China. Due to the differences in each index unit, we processed the data logarithmically in order to enhance the validity of this empirical study. Since there are boundaries around adjacent provincial regions, the K-Nearest Neighbors for Spatial Weights were used, as the K-Nearest Neighbor is a model with a changeable search distance. The K data-points closest to the center form a neighboring data-set. If the data are dispersed, the search distance becomes wider. In cases where the distribution of data in the studied area are scattered, the K-Nearest Neighbor can be used to ensure the existence of the adjacent object. As the neighbors of each provincial region are quite different in number, we use this matrix to ensure that each can find its neighbors within in certain distance. Given this, the weight of the geographic unit and its adjacent provincial regions is the reciprocal of their geometric distance, i.e., $\frac{1}{d_{ij}}$.

## **3. Analysis of Spatial Evolution Characteristics of Urban Pollution**

### *3.1. Analysis of Global Spatial Autocorrelation*

This paper uses Moran's I to explore the spatial correlation. In order to analyze the changes of $SO_2$, $NO_x$, and DUS emissions from 2011 to 2017, we statistically analyzed how the three pollutant emissions were distributed in each provincial region in 2011, 2014, and 2017. The spatial quartile distributions are shown in Figure 1.

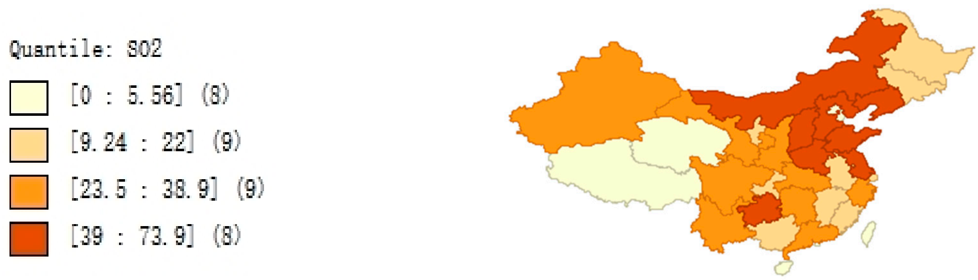


(2011)

**Figure 1.** *Cont.*

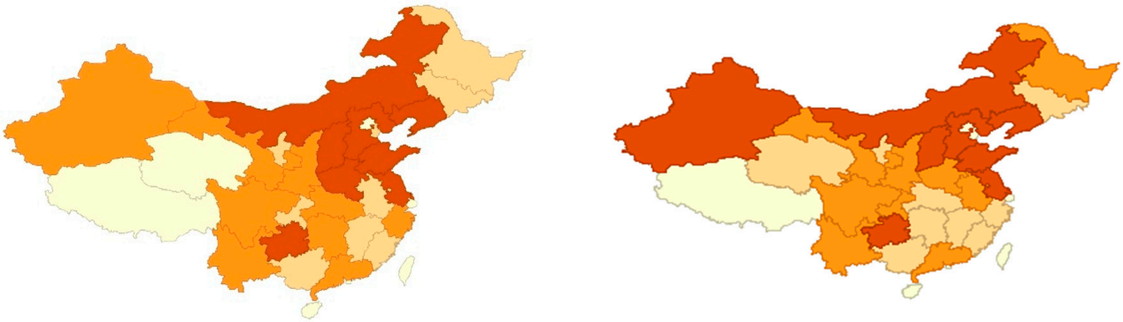

(2014) (2017)

**Figure 1.** Sulfur dioxide ($SO_2$) Emissions Distributions in China's provincial regions in 2011, 2014, and 2017.

As shown in Figure 1, the saturation of the orange color decreases in correlation with each region's decrease in $SO_2$ emission. Provinces in the dark orange area have the highest $SO_2$ emission and provinces in the cream cultured regions have the lowest $SO_2$ emission. In 2011 and 2014, the dark orange areas included Inner Mongolia, Liaoning, Shanxi, Hebei, Guizhou, Shandong, Jiangsu, and Henan. In 2017, the amount of $SO_2$ emission decreased in Henan, and yet increased in Xinjiang. In 2011 and 2014, excluding the increase in emissions in Tianjin, the cream-colored areas, the light orange and the orange areas remained unchanged. In 2017, $SO_2$ emissions in Heilongjiang, Chongqing, and Anhui increased, while those in Tianjin, Hunan, Hubei, and Zhejiang decreased.

As shown in Figure 2, provinces with the first grade of $NO_x$ emissions marked by dark orange remained unchanged in 2011, 2014, and 2017. These areas include: Inner Mongolia, Shanxi, Hebei, Liaoning, Shandong, Jiangsu, Henan, and Guangdong. Jilin Province experienced an increase of $NO_x$ emissions in 2014 and a decrease in 2017. Air pollution experienced a rebound in Jiangxi Province in 2017 after the decrease in 2014. In 2017 $NO_x$ particulate decreased in Shaanxi but increased in Guizhou.

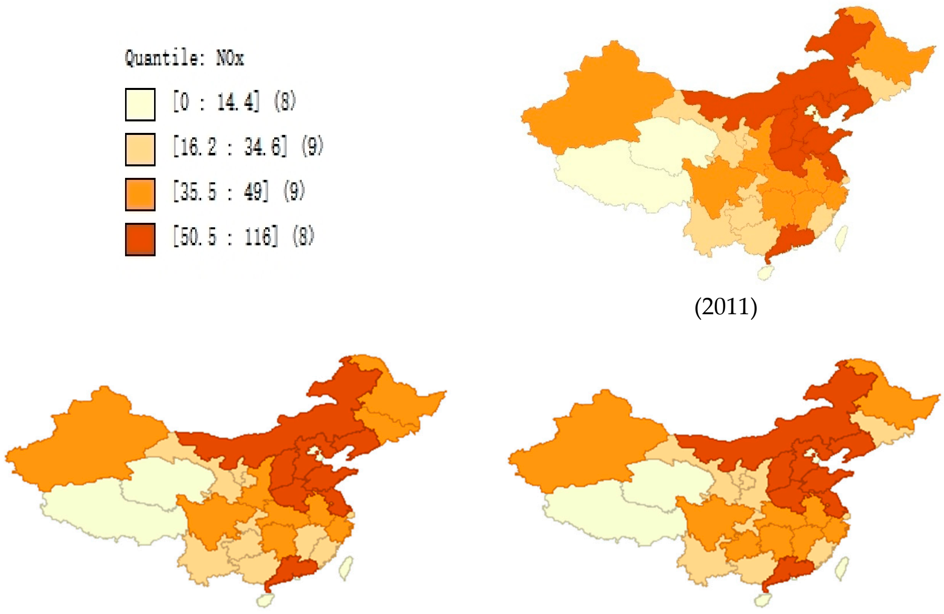


(2014) (2017)

**Figure 2.** Nitrogen oxides ($NO_x$) Emissions Distributions in China's provincial regions in 2011, 2014, and 2017.

As can be seen in Figure 3, the provinces with highest DUS emissions in 2011 and 2014 are marked by dark orange. These regions include: Xinjiang, Inner Mongolia, Heilongjiang, Shanxi, Hebei, Henan, Liaoning, Shandong, and Jiangsu. In 2017, DUS emissions in Henan decreased. After the decrease in Yunnan Province in 2014, it increased again in 2017. In 2017, emissions decreased in Jilin and Hubei, but increased in Guangxi and Jiangsu.

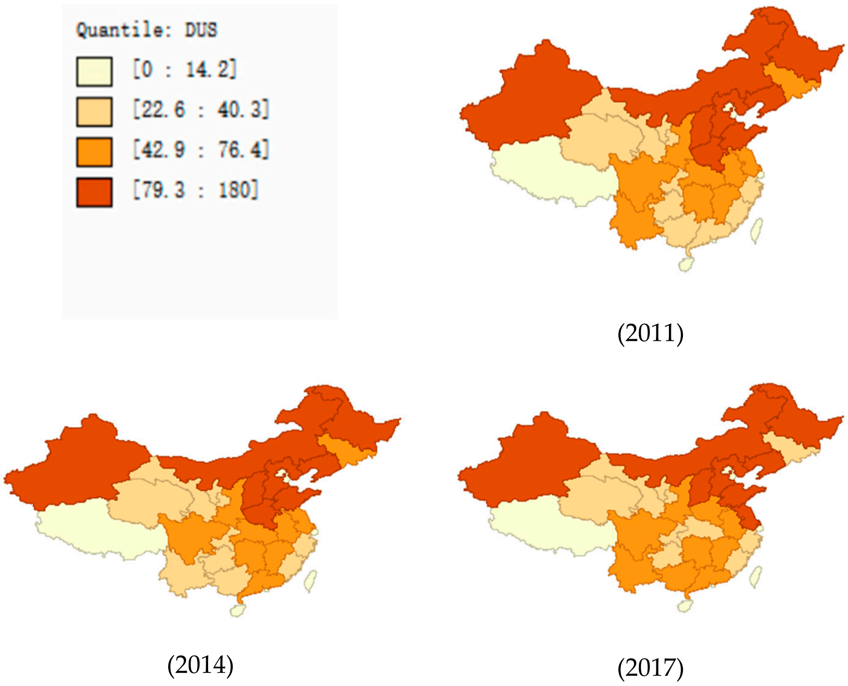


**Figure 3.** Smoke dust (DUS) Emissions Distributions in China's provincial regions in 2011, 2014, and 2017.

After assessing the data, a global spatial autocorrelation test was carried out. With this test, the present study draws Moran's I scatter plots of $SO_2$, $NO_x$, and DUS emissions in China's provinces in 2011, 2014, and 2017. The scatter plot includes global Moran's I. The distribution of the scatter points on the coordinate axis can visualize the cluster features of pollutants in different provinces, providing a clear way to demonstrate the empirical results. In Figure 4, the horizontal axis is pollutant emissions, and the vertical axis is spatial lagged term of the pollutant emissions, namely the weighted average of the adjacent values.

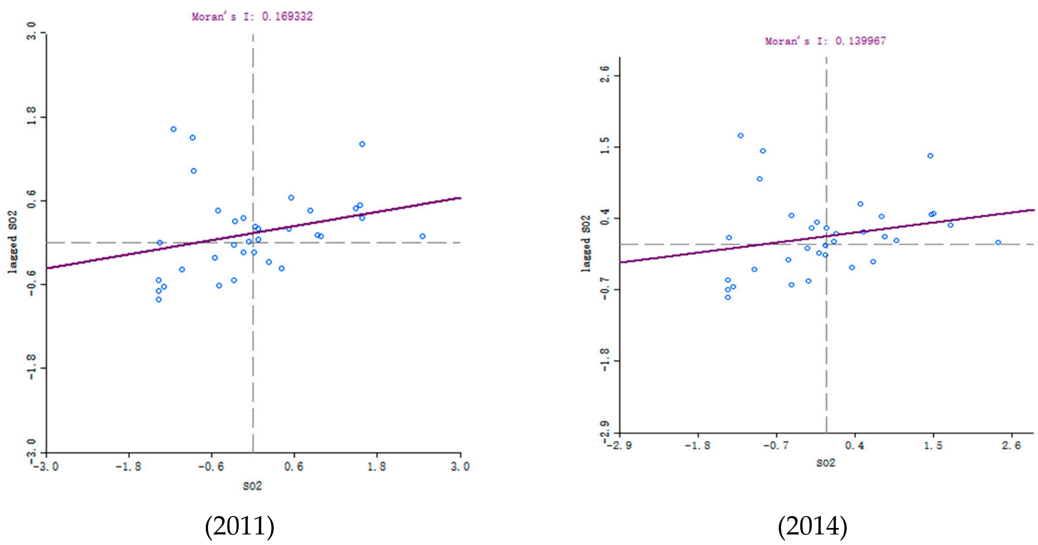


**Figure 4.** *Cont.*

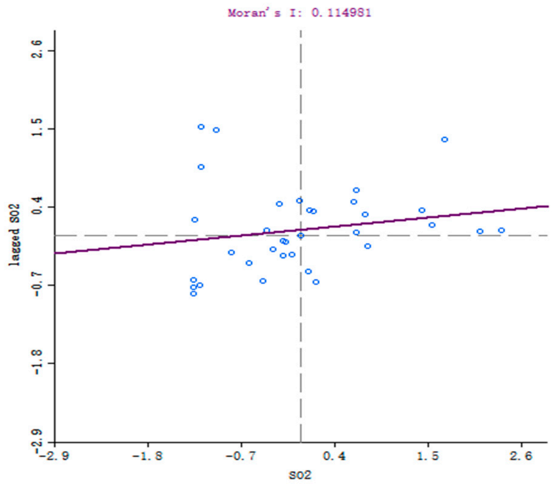


(2017)

**Figure 4.** Moran's I Scatter Plots of $SO_2$ Emissions in 2011, 2014, and 2017.

The scatter charts in Figure 4 shows the Moran's I of $SO_2$ emissions in China's provinces in 2011, 2014, and 2017 are 0.169332, 0.139967, and 0.114981, respectively, all of which are positive values, indicating that there is a positive correlation in $SO_2$ emissions among various provinces of China. As shown in Figure 4, most provinces' points are in the first and third quadrants, which indicates that provinces with high emissions tend to be surrounded by provinces with high air pollution, i.e., (H, H) cluster, and likewise, provinces with low emissions tend to be surrounded by other provinces with low emissions, i.e., (L, L) cluster. In these three years, the fourth quadrant distribution is the least of the four quadrants. These characteristics clearly show that provinces with higher $SO_2$ emissions tend to cluster, and provinces with lower $SO_2$ emissions also tend to cluster. Overall, $SO_2$ emissions in China present characteristics of cluster.

As can be seen from Figure 5, the Moran's I values of $NO_x$ emissions in China's provinces in 2011, 2014, and 2017 are 0.236313, 0.196591, and 0.200269, respectively, which are all above zero, indicating that $NO_x$ emissions present a positive correlation among various provinces. There are more provinces distributed in the first and third quadrants, which indicates that the $NO_x$ emissions in China's provinces are mainly characterized by (H, H) cluster and (L, L) cluster. The fourth quadrant distribution is the least among the four quadrants, indicating that $NO_x$ emissions has spatial cluster.

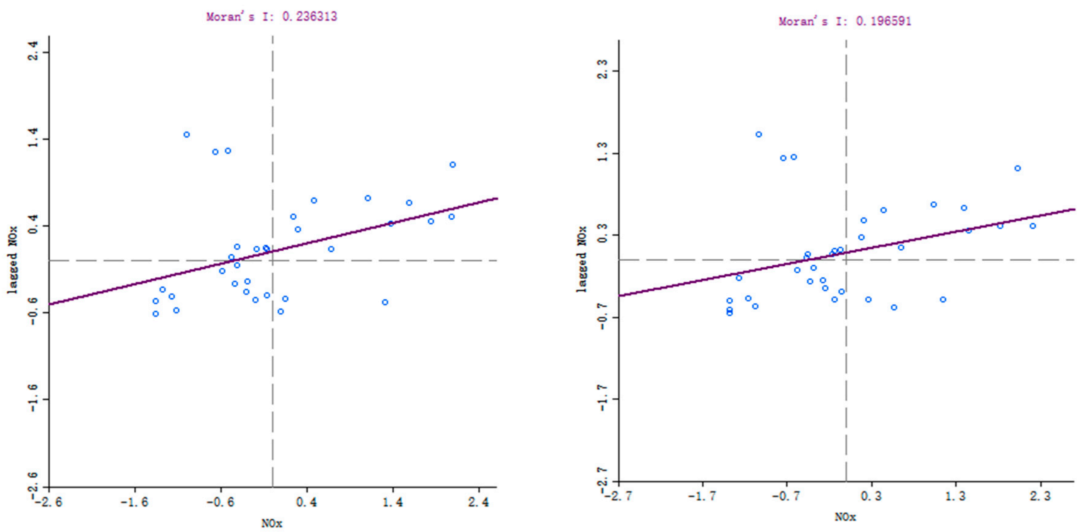


(2011) (2014)

**Figure 5.** *Cont*.

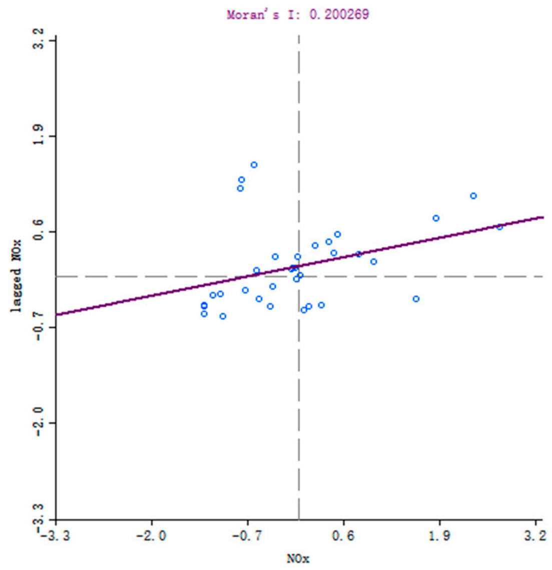


(2017)

**Figure 5.** Moran's I Scatter Plots of $NO_x$ Emissions in 2011, 2014, and 2017.

As evident from Figure 6, the Moran's I values of DUS emissions in China's provinces in 2011, 2014, and 2017 are 0.250947, 0.257236, and 0.19996, respectively, indicating that there is a positive correlation among DUS emissions in various provinces. The distribution of the first and third quadrants is relatively dense, which shows that the DUS emissions in China mainly presents (H, H) cluster and (L, L) cluster. The fourth quadrant distribution is the minimum of the four quadrants, meaning that $NO_x$ emissions take on a spatial cluster.

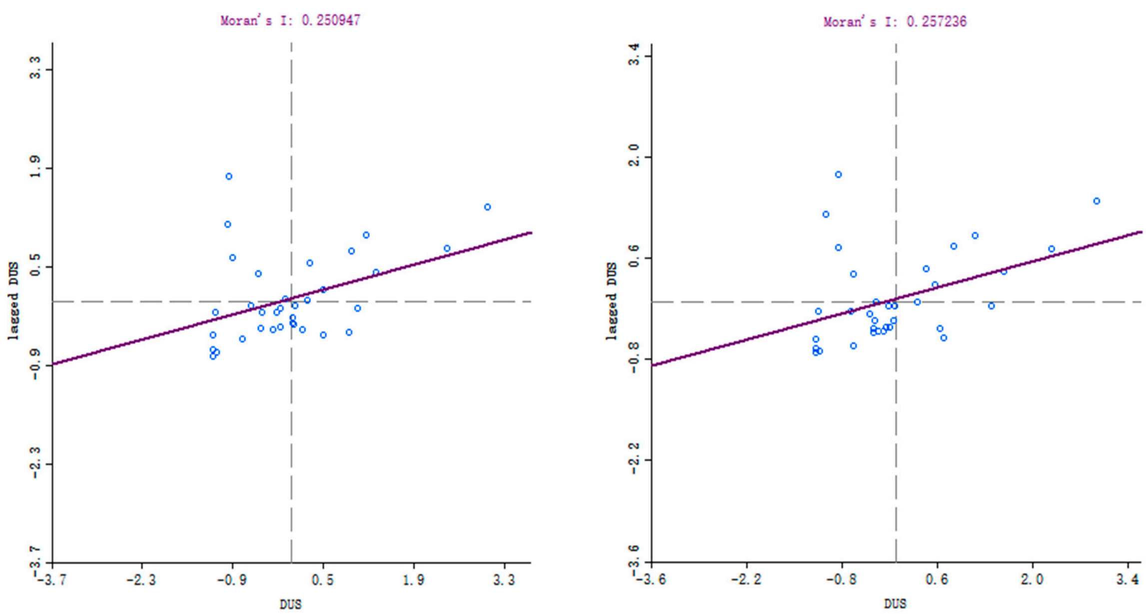


(2011) (2014)

**Figure 6.** *Cont.*

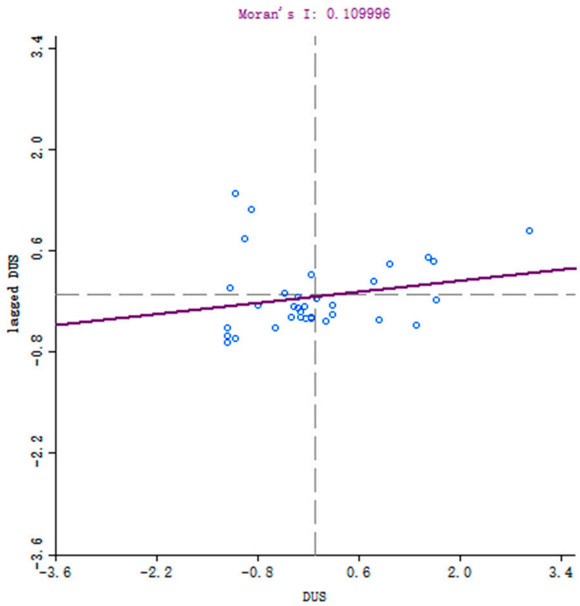


(2017)

**Figure 6.** Moran's I Scatter Plots of DUS Emissions in 2011, 2014, and 2017.

The scatter plot divides the relevant patterns of pollutant emissions into four types according to the coordinate system: the first quadrant on the upper right of the coordinates shows that areas with high pollutant emissions are clustered by other areas that also demonstrate high pollutant emissions. It means that the spatial correlation is positive and is represented by (H, H). The second quadrant on the upper left of the coordinates represents that areas with low pollutant emissions are surrounded by areas with high pollutant emissions, reflecting negative spatial correlation, which is represented by (L, H). The third quadrant on the lower left of the coordinates stands for regions with low pollutant emissions has the similar level of pollutant emissions in the neighboring regions, demonstrating a positive spatial correlation shown by (L, L). The lower right of the coordinates is the fourth quadrant, representing areas with pollutant emissions are characterized by low pollutant emissions in the adjacent areas, indicating that there is negative spatial correlation, i.e., (H, L). The spatial correlations in the first and third quadrants are positive, meaning that there is a dependency among similar geographic observation units; the spatial correlation in the second and fourth quadrants is negative, indicating that there is heterogeneity among different geographic observation units. As shown in the above figure, most of China's provinces are in the first and third quadrants, that is, they present the (H, H), (L, L) cluster and fewer provinces are in the second and the four quadrants, reflecting the non-homogeneous characteristics of (L, H) and (H, L). It can be concluded that the $SO_2$, $NO_x$, and DUS emissions in different regions of China have both the characteristics of spatial cluster and heterogeneity.

After analyzing the scatter charts, we calculated Moran's I of $SO_2$, $NO_x$, and DUS emissions in China's provinces from 2011 to 2016 and summarized them in the bar charts in 2.7. It can be seen that the Moran's I of $SO_2$ declines obviously, the Moran's I of $NO_x$ decreases year by year from 2011 to 2016, but rebounds in 2017, and the Moran's I of DUS experiences a large fluctuation, maintaining a low level in 2013, but increasing dramatically in 2014 and 2015 and rebounding to its lowest cluster of particles in seven years in 2017. In the past seven years, the Moran's I of the three pollutant emissions in each province has changed as shown by the line in Figure 7, and the overall trend is down-warding, indicating that the emissions of $SO_2$, $NO_x$, and DUS in China have been concentrated as a whole. Moreover, in the past seven years, the positive spatial correlation has shown an overall downward trend.

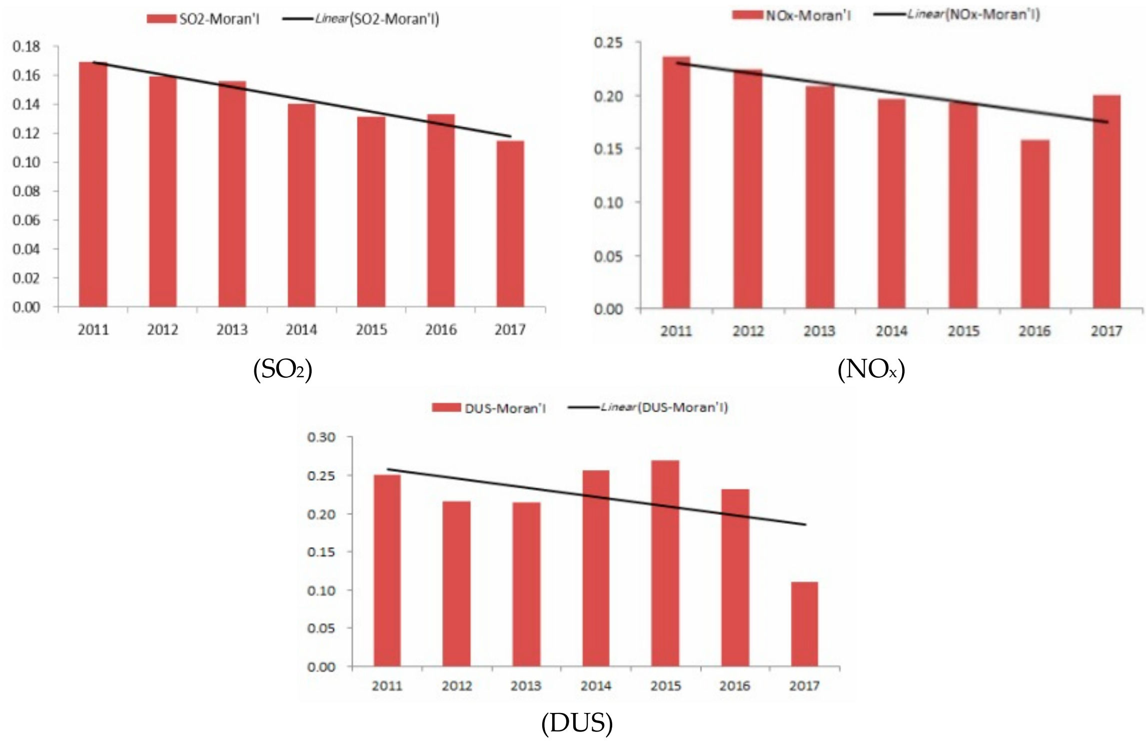


**Figure 7.** Bar Charts of Moran's I about three pollutants Emissions in Provinces in China from 2011 to 2017.

### *3.2. Analysis of Local Spatial Autocorrelation*

We used LISA cluster analysis to analyze $SO_2$, $NO_x$, and DUS emissions in 2011, 2014, and 2017, which allows us to observe more directly both the spatial dependency and heterogeneity of the emissions of the three pollutants from the cluster or dispersion of different colors in the local spatial effect maps.

Figure 8 shows spatial clustering distributions of $SO_2$. It can be seen that the clustering characteristics of $SO_2$ emissions remain unchanged in 2011, 2014, and 2017. Hebei Province is marked out by the red color, indicating that $SO_2$ emissions are very concentrated in the region. Similar to the previous analysis, it belongs to the (H, H) cluster. Beijing, Tianjin, and Shanghai appear in blue-violet, demonstrating the (L, H) cluster. This means that in 2011, 2014, and 2017, $SO_2$ emissions in Beijing, Tianjin, and Shanghai are lower, but are higher and more concentrated in their surrounding provinces. Most regions are gray. Shanghai and Beijing passed the 95% and 99.9% confidence intervals test, respectively, and Hebei and Tianjin passed the 99% confidence interval test. This indicates that $SO_2$ emissions in the gray areas have not yet formed a significant local correlation with their neighboring areas.

As can be seen from Figure 9, the spatial distribution characteristics of $NO_x$ in 2011 and 2014 are unchanged. In 2017, Shanxi Province changed from red to gray and Shandong Province changed from gray to red. Combined with Figure 2, we deduce that the reason might be that the neighboring province of Shanxi Province, Shaanxi Province, decreased its $SO_2$ emissions, and hence no (H, H) cluster was formed. Shandong Province was probably affected by its adjacent provinces like Hebei and Jiangsu, which were presented in the (H, H) clusters. Beijing, Tianjin, and Shanghai are shown in blue-violet, demonstrating the (L, H) cluster. This shows that in 2011, 2014, and 2017 $NO_x$ emissions were lower in Beijing, Tianjin, and Shanghai, but higher in their neighboring provinces, hence higher in terms of agglomeration. Most of the other regions are gray. Shanghai, Tianjin, and Beijing are significant at 0.01 significance levels, while Shandong, Hebei, and Jiangsu are significant at 0.05 significance levels.

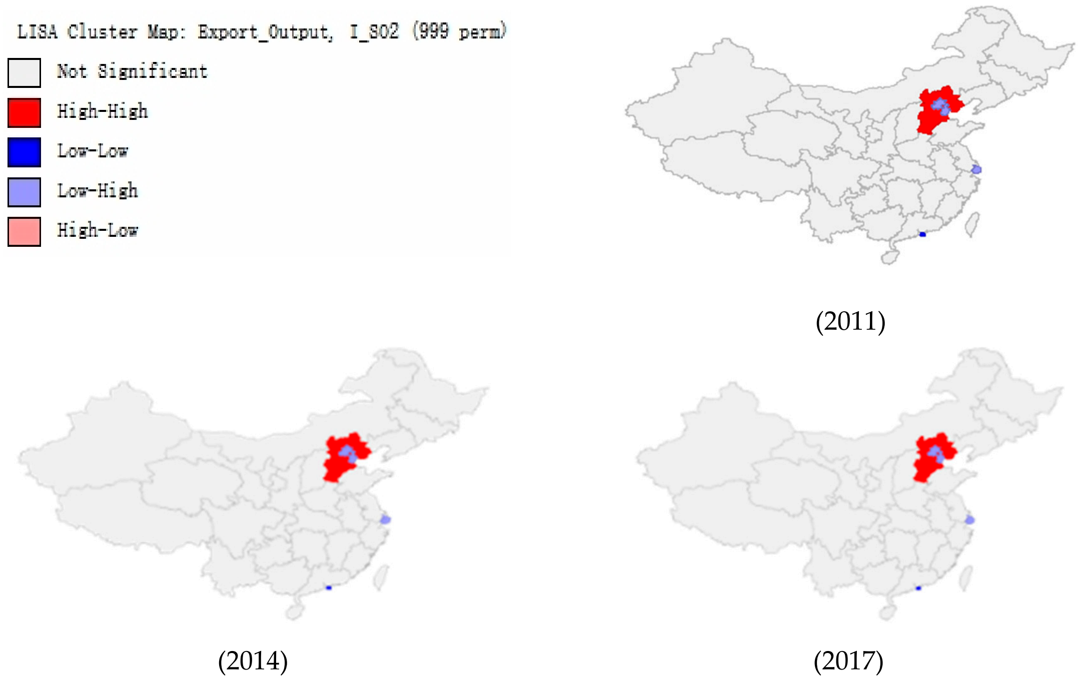


**Figure 8.** Local Indicators of Spatial Association Clustering Distributions of $SO_2$ Emissions in China's Provinces in 2011, 2014, and 2017.

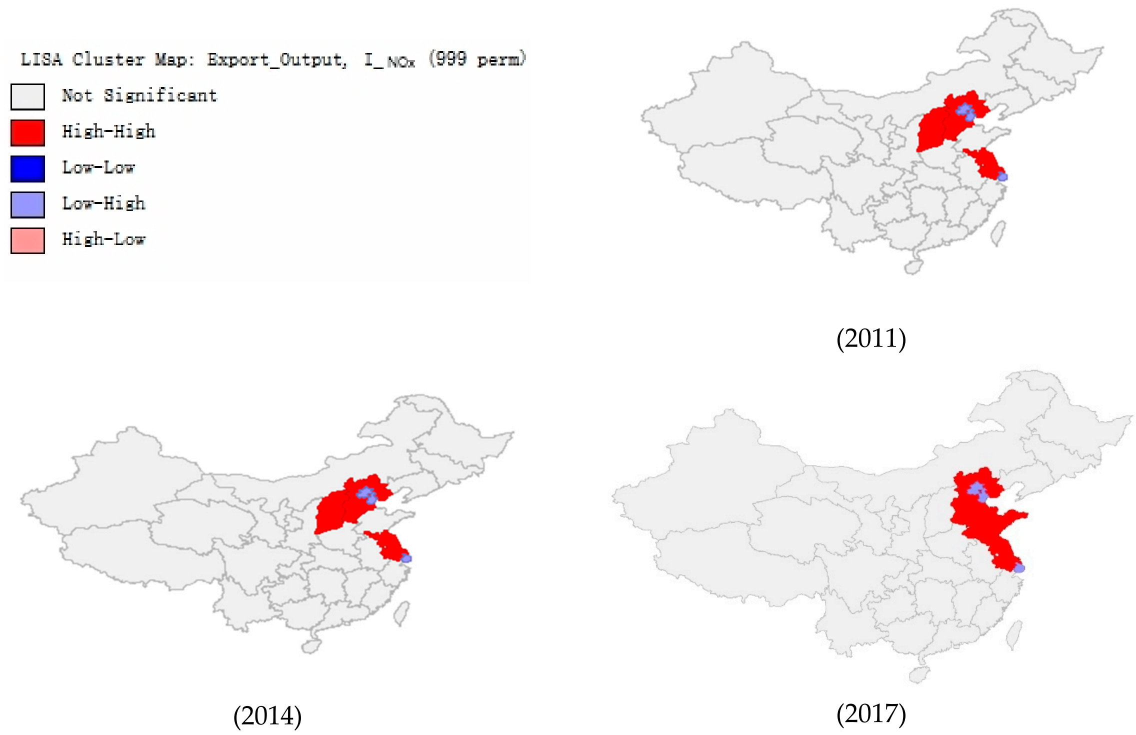


**Figure 9.** Local Indicators of Spatial Association Clustering Distributions of $NO_x$ Emissions in China's Provinces in 2011, 2014, and 2017.

It can be seen from Figure 10 that the distribution characteristics of DUS spatial clusters remain unchanged in 2011 and 2014. The number of regions with significant clustering characteristics decreased in 2017, and only Hebei Province presented (H, H) cluster. Inner Mongolia, Shanxi, Henan Province changed from red to gray. Combined with Figure 3, we estimate that the DUS emissions in Henan Province in 2017 decreased by 47.91% compared with that in the previous year, which has an impact on the clustering characteristics of Shanxi Province. It shows that the DUS emissions in Shanxi Province decreased by 36.35% compared with the previous year, affecting the (H, H) characteristics in Inner Mongolia. Beijing, Tianjin, and Shanghai are shown blue-violet in color, hence the (L, H) cluster. This indicates that $NO_x$ emissions of these three cities are similar to those of their surrounding provinces in three years. Shanghai passed the 95% confidence interval test, and Beijing, Tianjin, and Hebei passed the 99% confidence interval test.

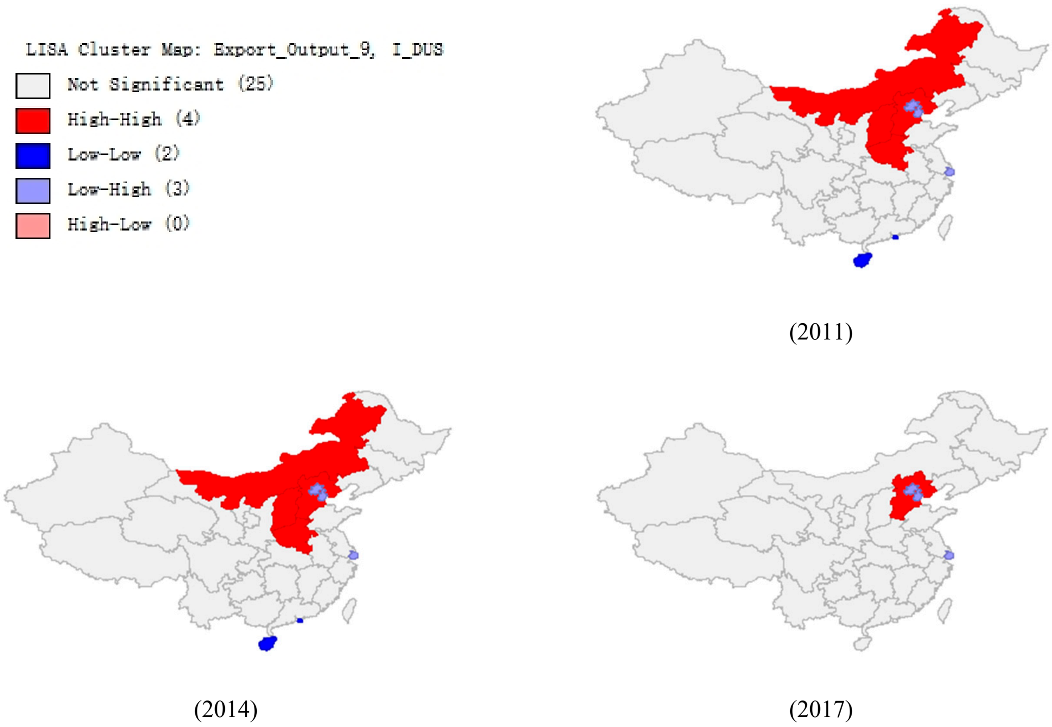


**Figure 10.** Local Indicators of Spatial Association Clustering Distributions of DUS Emissions in China's Provinces in 2011, 2014, and 2017.

## 4. Analysis of Factors Affecting the Spatial Evolution of Urban Pollution

In order to explore the factors influencing the spatial distribution of $SO_2$, $NO_x$, and DUS, we used MATLAB to estimate the SLM and SEM of the three pollutants, and thus to compare the results between the two. Tables 1 and 2 present all of the results.

**Table 1.** Maximum likelihood (ML) Estimation Results of Factors Affecting $SO_2$, $NO_x$, and DUS Emissions in the Spatial Lag Model (SLM).

| | **$SO_2$** | | **$NO_x$** | | **DUS** | |
|---|---|---|---|---|---|---|
| | **Regression Coefficients** | ***p* Value** | **Regression Coefficients** | ***p* Value** | **Regression Coefficients** | ***p* Value** |
| $\rho$ | 0.054999 | 0.406237 | 0.108970 | 0.116231 | 0.226989 | 0.002681 *** |
| *LnIND* | 2.644516 | 0.000000 *** | 1.469480 | 0.000000 *** | −50.689925 | 0.000389 *** |
| *LnURB* | 4.204875 | 0.000000 *** | 1.438522 | 0.000007 *** | 2.678510 | 0.000000 *** |
| *LnDEN* | −0.417434 | 0.000780 *** | −0.198740 | 0.032070 ** | −0.117083 | 0.399983 |
| *LnFDI* | 0.254323 | 0.000000 *** | 0.281015 | 0.000000 *** | 0.237579 | 0.000000 *** |
| *LnAGDP* | −3.246095 | 0.000000 *** | −1.458578 | 0.000000 *** | −2.327566 | 0.000000 *** |
| $R^2$ | 0.6587 | | 0.6035 | | 0.4370 | |
| *LogL* | −215.16349 | | −153.66707 | | −237.26945 | |
| *LM − test* | 0.0470 | 0.828 | 0.3230 | 0.570 | 1.3893 | 0.239 |
| *Robust LM − test* | 6.4067 | 0.011 | 6.8686 | 0.009 | 0.0479 | 0.827 |

* Correlation is significant at the 0.1 level (two-tailed); ** Correlation is significant at the 0.05 level (two-tailed); *** Correlation is significant at the 0.01 level (two-tailed).

**Table 2.** ML Estimation Results of Factors Affecting $SO_2$, $NO_x$, and DUS Emissions in the Spatial Error Model (SEM).

| | $SO_2$ | | $NO_x$ | | DUS | |
|---|---|---|---|---|---|---|
| | **Regression Coefficients** | ***p* Value** | **Regression Coefficients** | ***p* Value** | **Regression Coefficients** | ***p* Value** |
| $\lambda$ | 0.292995 | 0.000641 *** | 0.331990 | 0.000068 *** | 0.404993 | 0.000000 *** |
| *LnIND* | 2.661940 | 0.000000 *** | 1.410802 | 0.000000 *** | −42.744716 | 0.001308 *** |
| *LnURB* | 4.174688 | 0.000057 *** | 1.184057 | 0.000526 *** | 2.041079 | 0.165560 |
| *LnDEN* | −0.489710 | 0.000000 *** | −0.258437 | 0.004140 *** | −0.187663 | 0.000000 *** |
| *LnFDI* | 0.299076 | 0.000000 *** | 0.334682 | 0.000000 *** | 0.332826 | 0.000000 *** |
| *LnAGDP* | −3.327357 | 0.000000 *** | −1.497893 | 0.000000 *** | −2.344978 | 0.000000 *** |
| $R^2$ | 0.6548 | | 0.5911 | | 0.3824 | |
| *LogL* | −210.86564 | | −148.61153 | | −232.56495 | |
| *LM − test* | 6.2571 | 0.012 | 5.6355 | 0.018 | 2.2220 | 0.136 |
| *Robust LM − test* | 12.6169 | 0.000 | 12.1811 | 0.000 | 0.8806 | 0.348 |

* Correlation is significant at the 0.1 level (two-tailed); ** Correlation is significant at the 0.05 level (two-tailed); *** Correlation is significant at the 0.01 level (two-tailed).

The estimation results given in Tables 1 and 2 show the goodness of fit $R^2$ of the SLM and the SEM for $SO_2$ pollutant are 0.6587 and 0.6548, respectively. This indicates that the SLM and the SEM fit well. Spatial effect included, the model with maximum likelihood estimation can effectively avoid the deviation of results caused by the traditional Least Squares Estimation. As can be seen from the above table, Log-likelihood of the SLM is −215.16349, LM value is 0.0470, and *p* value is 0.828, greater than 0.1, hence failing the significance level test at the 90% confidence interval. Robust LM value is 6.4067, and *p* value is 0.011, passing the significance level test at 95%. Log-likelihood value of the SEM is −210.86564, which is greater than the Log-likelihood value of the SLM, LM value is 6.2571, and *p* value is 0.012, hence passing the significance level test at 95%. Robust LM value is 12.6169, and *p* value is 0.000, passing 99% confidence interval test. To avoid estimation errors, the multicollinearity among independent variables also had been tested. The results show that variance inflation factors (VIF) of all independent variables are below 10, indicating that there is no multicollinearity among independent variables. Hence, the results show that the Spatial Error Model is more optimal for the study of influencing factors of $SO_2$ pollutants. The explanatory coefficients in the model all passed the significance test at 99% confidence level, among which the industry location quotient, the urbanization rate and the amount of foreign direct investment are positively correlated with $SO_2$ emissions, with the urbanization rate most obvious. Population density and per capita GDP are negatively correlated with $SO_2$ emissions, and per capita GDP has a significant negative impact.

The $R^2$ values of SLM and SEM for $NO_x$ were 0.6035 and 0.5911, respectively, demonstrating that the fitting of the SLM is more optimal than the SEM. Log-likelihood value of the SLM is −153.66707, LM value is 0.3230, and *p* value is 0.570, which is less significant. Robust LM value is 6.8686, and *p* value is 0.009, passing the significance level test at 99%. Log-likelihood value of the SEM is −148.61153, which is bigger than that of the SLM, LM value is 5.6355, and *p* value is 0.018, considerably significant at 95%. Robust LM value is 12.1811, and *p* value is 0.000, extremely significant at 99% confidence interval test. The results show that when studying the influencing factors of $NO_x$ pollutant emissions, the SEM is more optimal as the explanatory variable coefficients in the model are all significant with a 99% confidence level. Except for the negative correlation between population density and per capita GDP and $NO_x$ emissions, other factors generate positive correlations, among which is the fact that the more industries that cluster together, the higher the $NO_x$ emissions.

The factors influencing $SO_2$ and $NO_x$ emissions are affected by both pollutants in the same direction, but the urbanization rate has stronger influence on $SO_2$ emissions than industry agglomeration. The IND is the most influential factor of $NO_x$ emissions. In addition, per capita GDP has a strong negative impact on $SO_2$ emissions.

The $R^2$ value of the SLM and SEM for DUS is 0.4370 and 0.3824, respectively, reflecting that the fitting of the SLM is more optimal than the SEM. Log-likelihood value of the SEM is −232.56495, higher than that of the SLM, which is −237.26945. LM value and Robust LM value of the SLM are 1.3893 and 0.0479, respectively. LM value and Robust LM value of the SEM are 2.2220 and 0.8806, respectively. This indicates that when studying the factors for DUS emissions, the SLM should be used as except for population density, the explanatory variables in the model are all significant at the level of 0.01. Industry agglomeration has a strong negative effect on the emissions of DUS, while urbanization rate and foreign direct investment have positive impact.

## 5. Discussion

This paper has explored the spatial evolution of urban pollution by analyzing the spatial distribution characteristics of $SO_2$, $NO_x$ and DUS emissions. Using spatial panel data model, we have empirically investigated these three pollutants in 30 provinces of China. We found that:

(1) The three pollutants show significant spatial cluster, but different pollutants show variation in areas: (1) $SO_2$ emissions are unchanged in 2011 and 2014 except in Tianjin, where $SO_2$ increases. In 2017, emissions in Heilongjiang, Chongqing, and Anhui increased, while those in Tianjin, Hunan, Hubei, and Zhejiang decreased. (2) The first-grade regions remained unchanged from 2011 to 2017, and some provinces like Jilin witnessed an increase in emission in 2014 and then decrease in 2017, and Jiangxi rebounded in 2017 after a decrease in 2014; in 2017, emissions decreased in Shaanxi, but increased in Guizhou. (3) Regarding DUS emissions, most of the first-grade regions remained unchanged from 2011 to 2017, except for Henan province, which witnessed a reduction in 2017. Moreover, in Yunnan province, the DUS emissions decreased in 2014 and then rebounded in 2017; in 2017, emissions decreased in Jilin and Hubei, and yet increased in Guangxi and Jiangsu.

(2) In recent years, different pollutants have shown different regional characteristics: (1) $SO_2$ emissions is red in Hebei Province, hence (H, H) cluster, it is blue and purple in Beijing, Tianjin, and Shanghai, hence (L, H) cluster; (2) $NO_x$ emissions in Shandong, Hebei, Jiangsu is red, presenting (H, H) cluster, and Beijing, Tianjin, and Shanghai present (L, H) cluster; (3) the areas showing significant clustering of DUS emission have reduced. It only presents (H, H) cluster in Hebei, and (L, H) in Beijing, Tianjin, and Shanghai.

(3) The influencing factors of $SO_2$, $NO_x$, and DUS emissions: $SO_2$ emissions are positively correlated with industrial location quotient, urbanization rate, and foreign direct investment amounts, with urbanization rates as the most obvious factor. $SO_2$, $NO_x$, and DUS emissions are negatively correlated with population density and per capita GDP, with the latter being particularly obvious. For $NO_x$, excluding the evidence that population density and per capita GDP are inversely correlated, other factors have a positive impact. Particularly, the stronger the industrial concentration, the higher the $NO_x$ emissions. As for DUS emissions, the explanatory variables, except for population density, are significant at the significance level of 0.01, reflecting that industrial clustering has a strong negative correlation on the DUS emission; while both urbanization rate and foreign direct investment have a positive correlation.

According to the results, major applications are as follows:

First, in general, the main pollution areas remain consistent geographically, and are persistently located in mostly western and northeastern regions and some parts of central China. In addition, all three pollutants exhibit significant high and low agglomeration in the same regions. As a result, the first step towards this problem is to track the source of the problem. Governments should enhance supervision and punishment on existing pollution sources, and through joint commitment and cooperation among neighboring regions, it should strengthen public awareness and education about the dangers and damage that result from pollution. Meanwhile, governments should also establish supervisory mechanisms among the general public. All of these measures should be taken to address the problem and safeguard the environment in an all-round way. In addition, governments should also work on reducing the emission of pollutants in congregated areas, and therefore, facilitate balancing ecological development among regions through policy guidance and industrial adjustment.

Second, a solid work should be carried out to manage the pollutants and promote coordinated and sustainable development of all regions. Industrial structure and urbanization have a considerably positive impact on $SO_2$ and $NO_x$ emissions, while these same aspects have a strong negative effect on DUS. Therefore, regions should comprehensively consider the severity of various pollutants and key influencing factors in their own regions so as to develop sound management plans to control pollutant emissions. To achieve effective results, it is also necessary to promote sustainable public transportation, and to increase monitoring of corporate engagement in environmental protection and sustainable development.

Third, focus should also be put on how to increase the proportion of tertiary industry and prevent "dirty industries" driven by foreign markets from thriving in China. Per capita GDP has a strong negative impact on $SO_2$, $NO_x$, and DUS emissions, and the economy of cities is negatively correlated with the emission of atmospheric pollutants. FDI, however, has a positive impact on all three pollutants, demonstrating that foreign investment, to some extent, aggravates urban pollution. Therefore, regions should readjust the existing development structure, deepen supply-side reform, accelerate the renewal of conventional industries, raise the proportion of the tertiary industry, and seek to substitute their original economic model of high pollution and high energy consumption with a model that does not flourish at the expense of the environment. Moreover, regions should also prevent foreign industries with high pollutions from moving their sites in. Other measures include adjusting urban ecological environments by increasing green spaces in cities and seeking sustainable development of cities.

## 6. Limitations and Prospects

By analyzing the three pollutants of $SO_2$, $NO_x$, and smoke dust, this paper has studied the spatial evolution of urban pollution along with its influencing factors and achieved some conclusions. However, there are still some limitations, which can be improved with more in-depth research.

(1) The data samples are still insufficient. Due to the incompleteness of the data from the statistical yearbook, this study only measured data for seven years. A follow-up study can add data from additional periods of time to observe dynamic changes. Additionally, pollutants can further be classified. For example, smoke and dust pollutants can be subdivided into PM10, PM2.5 and others according to international pollutant statistic standards. Future studies can specify the classification of pollutants and adopt international monitoring and statistic indicators to make their research results more comparable.

(2) The factors discussed can be more inclusive. The factors included in this paper have not covered all the influencing factors. Some are left out, such as educational factors. Some models can be more convincing when more factors are included. For example, future study may cover more factors that influence the generation of smoke dust. In the meantime, the scope of the study can be extended to distinguish the counteractive of different pollutants to different factors.

**Author Contributions:** M.L. organized this study, conducted the study design, and drafted the manuscript. Y.H. contributed to the study design, prepared datasets, performed the statistical analysis, and drafted the manuscript. M.H. contributed to the paper revision.

**Acknowledgments:** This study was financially supported by the Humanities and Social Sciences Youth Fund Project of the Ministry of Education (Project No. 18YJC630073); and the National Natural Science Youth Fund Project (Project No. 71802154).

**Conflicts of Interest:** The authors declare no conflict of interest.

## References

1. Lelieveld, J.; Evans, J.S.; Fnais, M.; Giannadaki, D.; Pozzer, A. The contribution of outdoor air pollution sources to premature mortality on a global scale. *Nature* **2015**, *525*, 367–371. [CrossRef] [PubMed]

2. Johanna, L.; Marie-Abele Catherine, B.; Baccarelli, A.A.; Petros, K.; Letizia, T.; Augusto, L.; David, S.; Pantel, V.; Schwartz, J.D. Epigenetic influences on associations between air pollutants and lung function in elderly men: The normative aging study. *Environ. Health Perspect.* **2014**, *122*, 566–572.
3. Li, L.; Qian, J.; Ou, C.Q.; Zhou, Y.X.; Guo, C.; Guo, Y. Spatial and temporal analysis of Air Pollution Index and its timescale-dependent relationship with meteorological factors in Guangzhou, China, 2001–2011. *Environ. Pollut.* **2014**, *190*, 75–81. [CrossRef] [PubMed]
4. Tang, A.; Zhuang, G.; Ying, W.; Hui, Y.; Sun, Y. The chemistry of precipitation and its relation to aerosol in Beijing. *Atmos. Environ.* **2005**, *39*, 3397–3406. [CrossRef]
5. Duan, F.K.; He, K.B.; Ma, Y.L.; Yang, F.M.; Yu, X.C.; Cadle, S.H.; Chan, T.; Mulawa, P.A. Concentration and chemical characteristics of PM 2.5 in Beijing, China: 2001–2002. *Sci. Total Environ.* **2006**, *355*, 264–275. [CrossRef] [PubMed]
6. Kim, K.; Rosenthal, J.E.; Christian, H.; Barry, L.; Stuart, G.; Richard, G.; Cynthia, R.; Kevin, C.; Jia-Yeong, K.; Kinney, P.L. Assessing ozone-related health impacts under a changing climate. *Environ. Health Perspect.* **2004**, *112*, 1557–1563.
7. Brunekreef, B.; Holgate, S.T. Air pollution and health. *Lancet* **2002**, *360*, 1233–1242. [CrossRef]
8. Qiu, H.; Yu, T.S.; Tian, L.; Wang, X.; Tse, L.A.; Tam, W.; Wong, T.W. Effects of Coarse Particulate Matter on Emergency Hospital Admissions for Respiratory Diseases: A Time-Series Analysis in Hong Kong. *Environ. Health Perspect.* **2012**, *120*, 572–576. [CrossRef]
9. Hoffmann, B. Air Pollution in Cities: Urban and Transport Planning Determinants and Health in Cities. *Integr. Hum. Health Urban Transp. Plann.* **2019**, *21*, 425–441.
10. Georgescu-Roegen, N. *The Entropy Law and the Economic Process*; Harvard University Press: Cambridge, MA, USA, 1971.
11. Goeller, H.E.; Weinberg, A.M. The age of substitutability or what do we do when the mercury runs out? *Sci. Public Policy* **1975**, *191*, 4228.
12. Dasgupta, P.; Heal, G.M. *Economic Theory and Exhaustible Resources*; Cambridge Books: Cambridge, MA, USA, 1985; Volume 14, p. 355.
13. Grossman, G.M.; Krueger, A.B. Environmental Impacts of a North American Free Trade Agreement. *Social Sci. Electr. Publ.* **1991**, *8*, 223–250.
14. Dinda, S. Environmental Kuznets Curve Hypothesis: A Survey. *Ecol Econ.* **2004**, *49*, 431–455. [CrossRef]
15. Ma, Y.R.; Ji, Q.; Fan, Y. Spatial linkage analysis of the impact of regional economic activities on PM2.5 pollution in China. *J. Clean. Prod.* **2016**, *139*, 1157–1167. [CrossRef]
16. Hao, Y.; Liu, Y.M. The influential factors of urban PM 2.5 concentrations in China: A spatial econometric analysis. *J. Clean. Prod.* **2016**, *112*, 1443–1453. [CrossRef]
17. She, Q.; Xia, P.; Qian, X.; Long, L.; Ning, W.; Min, L.; Jia, W.; Zhou, T.; Ji, H.; Xiang, W. Air quality and its response to satellite-derived urban form in the Yangtze River Delta, China. *Ecol. Indic.* **2017**, *75*, 297–306. [CrossRef]
18. Chen, B.; Yang, S.; Xu, X.D.; Zhang, W. The impacts of urbanization on air quality over the Pearl River Delta in winter: Roles of urban land use and emission distribution. *Theor. Appl. Climatol.* **2014**, *117*, 29–39. [CrossRef]
19. Fang, C.; Liu, H.; Li, G.; Sun, D.; Miao, Z. Estimating the Impact of Urbanization on Air Quality in China Using Spatial Regression Models. *Sustainability* **2015**, *7*, 15570–15592. [CrossRef]
20. Mark, H.; Abdullah, M.; Jianlin, H.; Kleeman, M.J. Resolving the interactions between population density and air pollution emissions controls in the San Joaquin Valley, USA. *J. Air Waste Manag. Assoc.* **2012**, *62*, 566–575.
21. Han, L.; Zhou, W.; Li, W.; Li, L. Impact of urbanization level on urban air quality: A case of fine particles (PM 2.5) in Chinese cities. *Environ. Pollut.* **2014**, *194*, 163–170. [CrossRef]
22. Yuan, X.; Mu, R.; Zuo, J.; Wang, Q. Economic Development, Energy Consumption, and Air Pollution: A Critical Assessment in China. *Human Ecol. Risk Assess. Int. J.* **2015**, *21*, 781–798. [CrossRef]
23. Jones, L.; Vieno, M.; Fitch, A. Urban natural capital accounts: Developing a novel approach to quantify air pollution removal by vegetation. *J. Environ. Econ. Policy* **2019**, 1–16. [CrossRef]
24. Dong, Z.J.; Nan, Y.L.; Yang, C.L.; Fei, L.; Yun, L.Z.; Zhen, Z.Q.; Si, M.X.; Fei, Z.Y.; Ying, C. Concentration Levels, Biological Enrichment Capacities and Potential Health Risk Assessment of Trace Elements in Eichhornia crassipes from Honghu Lake, China. *Sci Rep.* **2019**, *9*, 2431.

25. Li, F.; Zhang, J.D.; Liu, W.; Liu, J.; Huang, J.; Zeng, G. An exploration of an integrated stochastic-fuzzy pollution assessment for heavy metals in urban topsoil based on metal enrichment and bioaccessibility. *Sci. Total Environ.* **2018**, *644*, 649–660. [CrossRef]
26. Wang, Q.; Dai, H.N.; Wang, H. A Smart MCDM Framework to Evaluate the Impact of Air Pollution on City Sustainability: A Case Study from China. *Sustainability* **2017**, *9*, 911. [CrossRef]
27. Elhorst, J.P. Applied Spatial Econometrics: Raising the Bar. *Spat. Econ. Anal.* **2010**, *5*, 9–28. [CrossRef]
28. Liu, H.; Ma, W.; Qian, J.; Cai, J.; Ye, X.; Li, J.; Wang, X. Effect of urbanization on the urban meteorology and air pollution in Hangzhou. *J. Meteorol. Res.* **2015**, *29*, 950–965. [CrossRef]
29. Copeland, B.R.; Taylor, M.S. Trade, Growth, and the Environment. *J. Econ. Lit.* **2004**, *42*, 7–71. [CrossRef]
30. Lehmijoki, U.; Palokangas, T. Trade, population growth, and the environment in developing countries. *J. Popul. Econ.* **2010**, *23*, 1351–1370. [CrossRef]
31. Managi, S. International trade, economic growth and the environment in high- and low-income countries. *Int. J. Glob. Environ. Issues* **2006**, *6*, 320–330. [CrossRef]
32. Cho, H.S.; Choi, M.J. Effects of Compact Urban Development on Air Pollution: Empirical Evidence from Korea. *Sustainability* **2014**, *6*, 5968–5982. [CrossRef]
33. Hopkins, A.S. City Size, Density and Sectoral Structure: Exploring Urban Sustainability in the Regions. *Geophys. Res. Abstr.* **2010**, *12*, 11975.
34. Rydin, Y. Environmental dimensions of residential development and the implications for local planning practice. *J. Environ. Plan. Manag.* **1992**, *35*, 43–61. [CrossRef]
35. Na, L.L.; Sheng, Q.J.; Sheng, H.Y.; Li, W.; Jing, J.Z.; Yue, B. Analysis of the Spatial-temporal Pattern and Influence Factors of China's per Capita Household Carbon Emissions. *J. Nat. Resour.* **2016**, *31*, 1364–1377.
36. Anselin, L. Local Indicators of Spatial Association—LISA. *Geogr. Anal.* **1995**, *27*, 93–115. [CrossRef]
37. Anselin, L. Spatial Econometrics: Methods and Models. *Econ. Geogr.* **1988**, *65*, 3–7.
38. Engle, R.F. A general approach to lagrange multiplier model diagnostics. *J. Econom.* **1982**, *20*, 83–104. [CrossRef]